RAPID COMMUNICATIONS

PHYSICAL REVIEW B VOLUME 51, NUMBER 17 1 MAY 1995-I

Distribution of magnetic flux in high-T_c grain-boundary junctions enclosing hexagonal and triangular areas

J. R. Kirtley, P. Chaudhari, M. B. Ketchen, N. Khare, Shawn-Yu Lin, and T. Shaw
IBM Thomas J. Watson Research Center, P.O. Box 218, Yorktown Heights, New York 10598
(Received 9 November 1994; revised manuscript received 13 February 1995)

We report here scanning superconducting quantum interference device microscope measurements of the magnetic-flux-threading grain-boundary junctions that completely enclose hexagonal and triangular regions. While the total flux through one of these junctions is $n\Phi_0$, there are distinct areas of localized flux with magnitudes much less than Φ_0. We present the experimental results and discuss possible explanations for these observations.

Conventional superconductors[1] as well as high-T_c superconductors[2] quantize flux in units of $\Phi_0=h/2e$. Recently evidence for a quantization of the form $(n+\frac{1}{2})\Phi_0$ for special high-T_c superconducting quantum interference device (SQUID), ring and junction structures has been reported.[3–10] We report in this paper observations of highly localized bundles of flux with magnitudes much less than a flux quantum in high-T_c grain boundaries. Our experiments were performed with a scanning SQUID microscope[11–14] on photolithographically produced grain-boundary samples. The SQUID microscope scans a small pickup loop of a low-T_c SQUID (Ref. 15) relative to the sample. The SQUID measures the magnetic flux through the pickup loop with noise of order $2\times10^{-6}\Phi_0/\mathrm{Hz}^{1/2}$, where the superconducting flux quantum $\Phi_0=h/2e=2.07\times10^{-7}$ G cm^2. The pickup loop is part of an integrated SQUID sensor which is fabricated on a silicon wafer. Magnetic-field resolution and sensitivity are optimized when the loop is as close to the sample as possible. This is done by polishing the silicon substrate to a sharp corner about a loop diameter from the center of the pickup loop, and scanning the sample relative to the SQUID with this point in contact with the sample at a shallow angle. In this geometry our 10 μm pickup loop samples primarily the normal component of the field about 2 μm above the plane of the sample. The fabrication and characterization of the photolithographically produced grain-boundary samples used in this experiment have been described elsewhere.[16,17] Briefly, an epitaxial film of MgO is grown onto a $LaAlO_3$ single-crystal substrate, and patterned to obtain the desired geometrical shape. An epitaxial film of CeO_2 is followed by a 250-nm-thick film of the superconductor $YBa_2Cu_3O_{7-x}$. The epitaxial growth of this system is such that the orientation difference between $YBa_2Cu_3O_{7-x}$ grown on and off the MgO is a rotation about the c axis of 45°. Verification of the crystalline orientations and quality of the grain boundaries has been made using various techniques,[17] including transmission electron microscopy. The critical current density of the grain boundaries, measured by transport techniques, is about 2×10^3 A/cm^2 at 4.2 K.

The basic Josephson relation for the supercurrent across a weak link between two superconductors is given by $I=I_c\sin\phi$, where ϕ is the superconducting order parameter difference. For an isotropic s-wave superconductor, I_c is independent of the orientation of the weak link boundary. For a d-wave superconductor with our geometry I_c is expected to be proportional to $(\cos^2\theta-\sin^2\theta)(\cos^2\theta'-\sin^2\theta')$,[5] where $\theta=\theta'-\pi/4$ is the angle between the normal to the interface and a crystalline symmetry (a or b) axis in the $YBa_2Cu_3O_{7-x}$. For a superconducting loop of inductance L with one weak link and $2\pi L|I_c|/\Phi_0>1$, spontaneous flux generation with value $\Phi_0/2$ has been predicted if the junction I_c is less than zero.[5] Our samples are enclosed grain boundaries with distributed supercurrents and inductances, so that comparison with a discrete model must be done carefully. For example, the individual corners of our hexagonal and triangular grain-boundary samples can be treated independently only as long as they are separated by distances longer than the Josephson penetration depth, and if the vortex-vortex coupling energies are small compared with other energies in the problem. In fact, the sides of the triangles and hexagons studied here (20–30 μm) are comparable to the Josephson penetration depth (~10 μm), and a typical vortex-vortex interaction energy ($\sim\Phi_0^2/2\mu_0 d\sim0.3$ eV) is comparable to the Josephson coupling energy ($I_c\Phi_0/2\pi\sim0.3$ eV). Nevertheless, crude estimates of the parameters can be made as follows: We estimate that the inductance per unit length of our grain boundaries is about 0.3 pH/μm, or about 6 pH for a side of our hexagons of length 20 μm. The supercurrent per unit length is about 6 μA/μm, or about 0.12 mA for the same length. If we take the effective grain-boundary length associated with a corner of a hexagon to be 20 μm, then the figure of merit $2\pi L_s I_c/\Phi_0$ is about 2. For some of our hexagonal grain-boundary samples material was removed by laser ablation from an area 10 μm^2 at the corners. The inductance of a square hole $d=10$ μm on a side is $L_h\sim1.25\mu_0 d\sim16$ pH, increasing $2\pi I_c(L_h+L_s)\Phi_0$ to about 8. Therefore the criterion $2\pi LI_c/\Phi_0>1$ is met, if only by a small margin. For comparison, the rings in the tricrystal grain-boundary experiments of Tsuei *et al.*,[9] where the half-integer flux quantum effect was directly observed, had $2\pi I_c L/\Phi_0\sim600$. Millis[18] has performed an analysis of the distribution of flux expected in an enclosed grain boundary between d-wave superconductors. He predicts spontaneous generation of vortices with $\pm\Phi_0/2$ flux in the grain boundaries, with a spatial extent perpendicular to the grain boundary of about the London

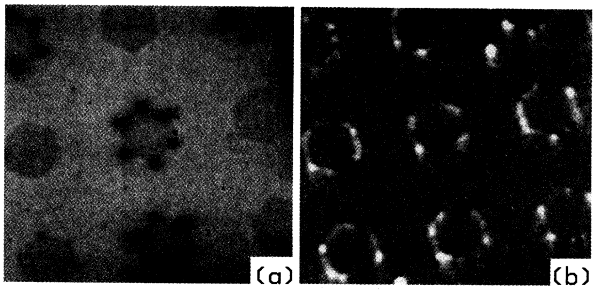

FIG. 1. Photograph of region 340×260 μm of an array of hexagonal grain boundaries (a), and scanning SQUID microscope image of the normal component of the magnetic field of this region. The samples were cooled in nominal zero field through the superconducting transition temperature of 90 K at a rate of 50 mK/s. Similar results were obtained for cooling rates as low as 10 mK/s. This grey-scale image has a full scale range of $0.25\Phi_0$ threading the sensor pickup loop (corresponding to a range in field of about 40 mG).

penetration depth ($\lambda \sim 1500$ Å in our case), and parallel to the grain boundary of 3–4 times the Josephson penetration depth[19] ($\lambda_j \sim 7$ μm for the overlapping planes geometry of Ref. 19, ~13–15 μm when corrected for the actual edge-on planes geometry of the sample). In contrast, we observe flux concentrations with much smaller total flux that is much more highly localized than predicted.

Figure 1(a) shows a photograph of an area 340×260 μm with a number of photolithographically produced hexagonal grain boundaries visible. The superconducting $YBa_2Cu_3O_{7-x}$ has been removed by laser ablation from 10 μm squares at the corners of four of the hexagons to increase the value of the inductance enclosed by loops around the corners. Figure 1(b) shows scanning SQUID images of the normal component of the field above the same area cooled in nominal zero field. Visible in Fig. 1(b) are two bulk vortices, one in the upper right quadrant of the image, and the second at the lower left edge. The edges of the hexagons are decorated with flux concentrations of both signs. They are apparently as localized as the bulk vortices, but have much smaller amplitudes. Also apparent in this image is much higher magnetic "noise" outside the hexagons vs inside them. This structure is quite repeatable from scan to scan in a particular cooldown, and is of uncertain origin. The full grey-scale variation in Fig. 1(b) is a $0.25\Phi_0$ change in flux through the pickup loop, corresponding to a field change of about 38 mG at the surface. Despite extensive efforts to cool slowly in zero field, we always observed some flux trapped in our grain boundaries, often with both signs. The positions of the trapped vortices varied from cooldown to cooldown and from hexagon to hexagon, and the positions of the trapped vortices could be moved within a given hexagon by applying an external field, generating screening currents, which drove the vortices by Lorentz forces. These effects are not peculiar to a hexagonal geometry: Figure 2 shows the same measurement, with the same grey-scaling, for an area with photolithographically patterned triangles. One possible explanation of the small nonquantized amplitudes is that the observed flux concentrations are actually a consequence of screening currents flowing in the films, but not across grain boundaries, to compensate for magnetic gradients. The fact

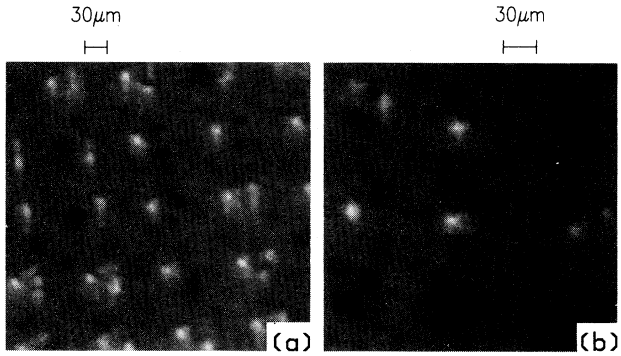

FIG. 2. Scanning SQUID micrographs of the magnetic field above the region of an array of triangular grain boundaries without (a) and with (b) superconducting material removed between the triangles [as indicated by the contrasting lines in (b)] to try to limit the effects of screening currents.

that these patterns do not simply scale in intensity as applied field is varied would be expected since the spatial variation of magnetic fields for this case would not be the same as for those locked in the sample during the superconducting transition. The area in Fig. 2(b) had superconducting material removed in a cross-hatched pattern between the triangles in an attempt to reduce the effects of screening of any residual field that might be present in the sample.

Figure 3 shows that we can model the flux from superconducting vortices trapped in the bulk of $YBa_2Cu_3O_{7-x}$ very well. Figure 3(a) is an image of an isolated flux quantum. Superposed on this image is the outline of the pickup loop, properly scaled and oriented. The image of a point source like a bulk vortex is determined by the geometry of the pickup loop. The "tail" in this image is due to excess pickup area from unshielded leads to the pickup loop. The dots in Fig. 3(b) are cross sections through the data as indicated by the contrasting lines in the image. The solid lines come from modeling the vortex as a magnetic monopole

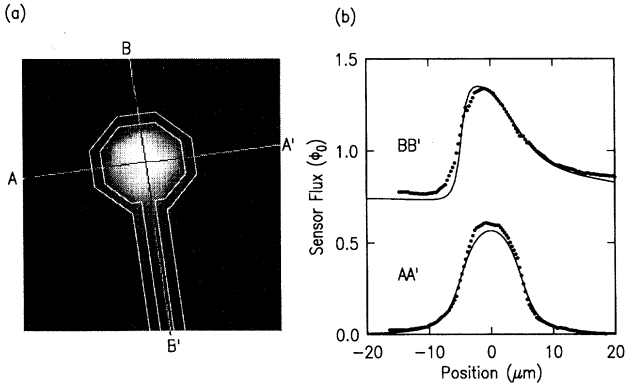

FIG. 3. (a) Abrikosov vortex trapped in the bulk of a thin film of $YBa_2Cu_3O_{7-x}$. The cross sections (dots) in (b) (the flux through the sensor loop as a function of position) are fit by assuming a total flux in the vortex of $\Phi_0 = h/2e$, with the spacing between the loop and the point of contact of the SQUID assembly as the only fitting parameter. In this geometry a bulk flux quantum (with total flux Φ_0) couples a total flux of about $0.6\Phi_0$ into the sensor loop of the SQUID.

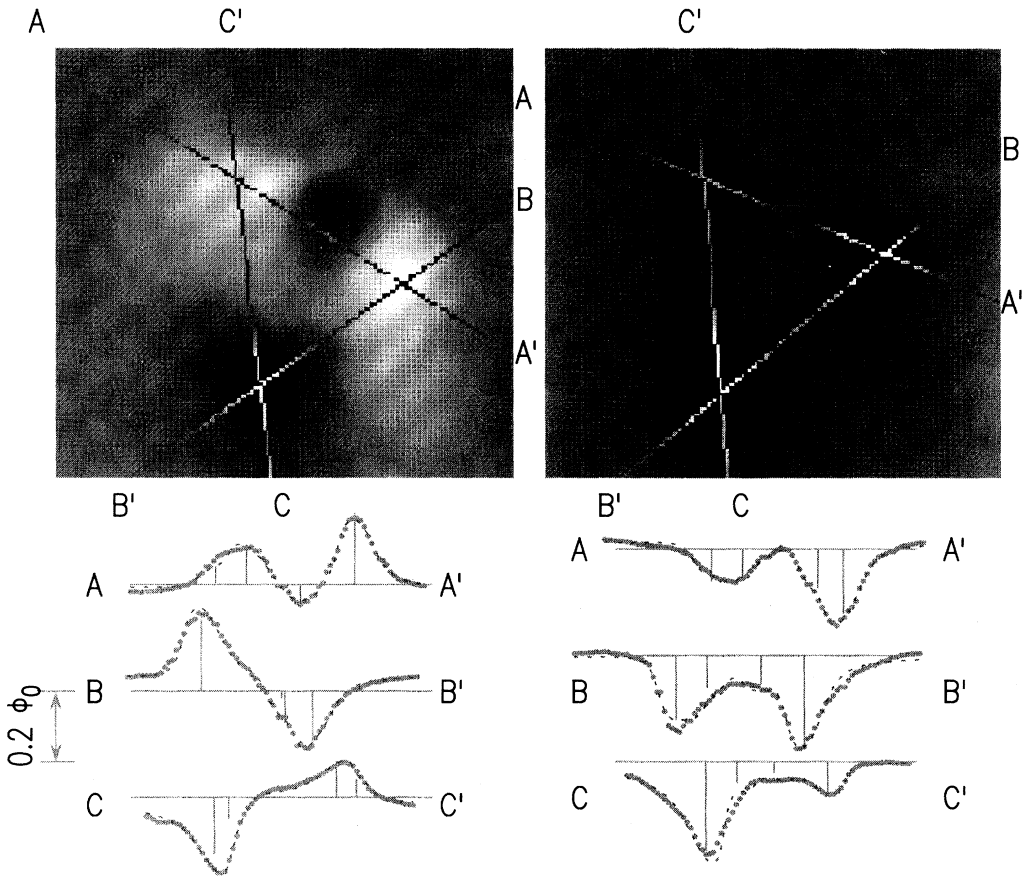

FIG. 4. The data from row 1, column 1 (left) and row 1, column 3 from Fig. 2(b) is fit using nine fractional flux vortices, each with total flux much smaller than Φ_0. The sum of the fractional charges in the left-hand fits is $0.05\Phi_0$, the sum for the right-hand fits is $-0.96\Phi_0$.

field source with $\mathbf{B}(\mathbf{r}) = \Phi_0 \mathbf{r}/2\pi|r|^2$, and integrating over the known geometry of the pickup loop, with the distance between the center of the pickup loop and the point where the SQUID assembly contacts the sample used as the only fitting parameter. The value obtained for this parameter, 8 μm, is in reasonable agreement with microscopic inspection of the SQUID assembly.

Figure 4 shows the results from a similar fitting procedure, keeping the loop-center to tip distance fixed at 10 μm, a value consistent with microscopic inspection of the SQUID assembly at the time, for two of the triangular grain boundaries in Fig. 2(b). Amplitudes and positions of δ function flux concentrations were used as fitting parameters for each triangle as follows: Four amplitudes and positions were used for each of the three cross sections for each triangle. The fits were optimized for one cross section, and the amplitude of an end-point fit flux concentration was carried over as a fixed parameter in the fit of the next cross section. The procedure was iterated around the triangle until convergence was reached. There were therefore only nine free fitting amplitudes, since each cross section shared one flux amplitude at a corner with the next cross section. The vertical lines in the lower part of Fig. 4 represent the positions and amplitudes of the fit flux concentrations, with lengths proportional to amplitude as indicated by the scaling bar. Naturally, with 18 fitting parameters the fits (solid lines) to the data (dots) in the lower part of Fig. 4 are very good. A large number of parameters were used to ensure that as little flux as possible was missed in the fitting procedure, to determine whether the sums added to integer multiples of a flux quantum. The same qualitative conclusions result when, for example, six fit amplitudes and positions are used. The remarkable thing about these fits is that the flux concentration amplitudes required are much smaller than the flux quantum Φ_0. Similarly striking, the fits are very good if we take the flux sources to be point sources, but are much worse if we take the sources to have spatial widths ~ 15 μm, the Josephson penetration depth: the concentrations are much more localized than one would expect for Josephson vortices, which are expected to be several λ_j wide.

Figure 5(a) shows a histogram of flux amplitudes for the 81 fitted amplitudes resulting from fitting the nine triangles in Fig. 2(b). The amplitudes are randomly distributed about a mean value slightly less than 0, indicating that a small field (~ 1 mG) was present while cooling the sample. A similar histogram for the sums of the flux amplitude fits for a particular triangle [Fig. 5(b)] come out either close to 0, or close to $-\Phi_0$. Apparently some of the total flux in the triangles is missed by our fitting procedure, since the lower sum peak is centered about $-0.85\Phi_0$. Nevertheless, Fig. 5(b) indicates

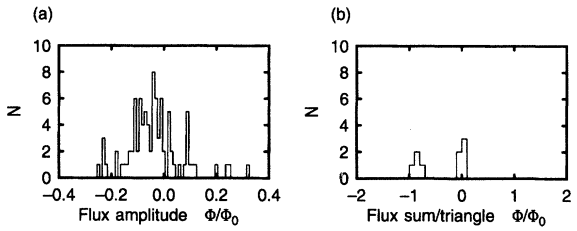

FIG. 5. Histograms of the number of occurrences of a particular fit flux amplitude (a) and sum of flux amplitudes for a particular triangle (b) from fitting 81 amplitudes to the nine triangles of Fig. 2(b).

that the conventional flux quantization condition is met for a triangle as a whole, if not for the individual concentrations of flux.

Our measurements leave us with two puzzling observations. The first is that the localized flux concentrations in the grain boundaries have amplitudes smaller than predicted, i.e., $\pm\Phi_0/2$ for a d-wave superconductor with our geometry. The second is that these concentrations are much more localized than expected. Sigrist *et al.*[20] have suggested that the small flux concentration amplitudes we observe may be due to breaking of time inversion symmetry in the grain boundaries. This is an exciting possibility, but other explanations must be carefully considered. One consideration to keep in mind is that these samples have relatively low Josephson coupling energies, so that the product $2\pi I_c L$ is not much lrager than Φ_0. Simple modeling shows that the ground state of a ring with a Josephson junction with a negative critical current (a π-ring) has substantially less than $\Phi_0/2$ spontaneous magnetization if $2\pi I_c L \sim \Phi_0$. For example, a spontaneous magnetization of magnitude $0.3\Phi_0$ would appear in a π-ring with $2\pi I_c L/\Phi_0 = 2$. However, this would not explain why small amplitude flux bundles appear at all corners, and sometimes in the edges, of the triangles. It might be argued that the flux has to be localized to some extent, since the circulating supercurrents are constrained by the geometry of the grain boundaries. Millis[18] has suggested that spatial nonuniformities in the grain boundary could result in a characteristic length scale shorter than the physical dimensions. However, it is difficult to understand how length scales shorter than the Josephson penetration depth can result if there is substantial current flow across the grain boundaries. As mentioned previously, the small nonquantized amplitudes may result from screening currents flowing in response to magnetic-field gradients. The images show no signature of a uniform gradient as would be expected from an externally applied field, although gradients generated by currents locked into other parts of the sample during the cooldown transient could also play a role.

An interesting alternative analogy to consider[21] is that of a quantum-mechanical one-dimensional multiwell system. A particle in such a system with energy greater than the interwell height will have a probability amplitude shared among multiple wells. The amplitude in any given well will not be quantized, but the sum of the probabilities of being in the wells will add up to unity. Perhaps the grain boundary can be thought of as providing a series of coupled potential wells for trapping flux with varying depth, so that the total quantized flux is distributed around it. With this explanation, however, it is hard to understand how the individual wells can be sufficiently tightly coupled to share flux, and yet not generate enough supercurrent between them to show substantial flux between the wells.

The scanning SQUID microscope used for this work was developed under the auspices of the Consortium for Superconducting Electronics. One of us (N.K.) thanks the U.S. International Agency and the Department of Science and Technology (Government of India) for a financial support under the Indo-U.S. Science and Technology Program. We would like to acknowledge the capable technical assistance of J. A. Lacey, and thank W. J. Gallagher and J. Z. Sun for providing the sample from which the image of Fig. 3 was taken.

[1] B. S. Deaver and W. M. Fairbank, Phys. Rev. Lett. **7**, 43 (1961).
[2] P. L. Gammel *et al.*, Phys. Rev. Lett. **59**, 2952 (1987); C. E. Gough *et al.*, Nature **326**, 855 (1987).
[3] V. B. Geshkenbein, A. I. Larkin, and A. Barone, Phys. Rev. B **36**, 235 (1978).
[4] W. Braunisch *et al.*, Phys. Rev. Lett. **68**, 1908 (1992).
[5] Manfred Sigrist and T. M. Rice, J. Phys. Soc. Jpn. **61**, 4283 (1992).
[6] F. V. Kustmartsev, Phys. Rev. Lett. **69**, 2268 (1992).
[7] D. A. Wollman *et al.*, Phys. Rev. Lett. **71**, 2134 (1993); D. A. Wollman *et al.*, *ibid.* **74**, 798 (1994).
[8] D. A. Brawner and H. R. Ott, Phys. Rev. B **50**, 6530 (1994).
[9] C. C. Tsuei *et al.*, Phys. Rev. Lett. **73**, 593 (1994).
[10] A. Mathai *et al.* (unpublished).
[11] F. P. Rogers, Master's thesis, MIT, 1983.
[12] L. N. Vu and D. J. van Harlingen, IEEE Trans. Appl. Supercond. **3**, 1918 (1993).
[13] R. C. Black *et al.*, Appl. Phys. Lett. **62**, 2128 (1993).
[14] J. R. Kirtley *et al.*, Appl. Phys. Lett. **66**, 1138 (1995).
[15] S. Bermon, J. M. Jaycox, and M. B. Ketchen, IBM Tech. Discl. Bull. **27**, 5847 (1985); M. B. Ketchen *et al.*, IEEE Trans. Appl. Supercond. **3**, 1795 (1993).
[16] K. Char, M. S. Colclough, S. M. Garrison, N. Newman, and G. Zaharchuk, Appl. Phys. Lett. **59**, 733 (1991).
[17] P. Chaudhari and Shawn-Yu Lin, Phys. Rev. Lett. **72**, 1084 (1994).
[18] A. J. Millis, Phys. Rev. B **49**, 15 408 (1994).
[19] C. S. Owen and D. J. Scalapino, Phys. Rev. **164**, 538 (1967).
[20] M. Sigrist, D. Bailey, and R. B. Laughlin, Phys. Rev. Lett. (to be published).
[21] Goran Wendin (private communication).

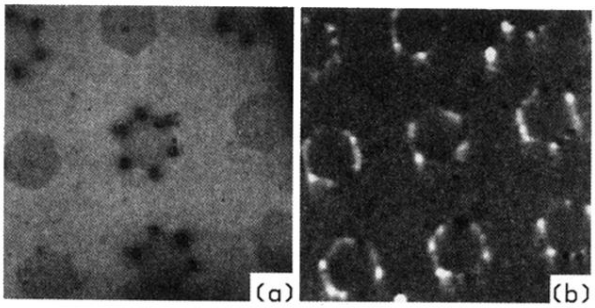

FIG. 1. Photograph of region 340×260 μm of an array of hexagonal grain boundaries (a), and scanning SQUID microscope image of the normal component of the magnetic field of this region. The samples were cooled in nominal zero field through the superconducting transition temperature of 90 K at a rate of 50 mK/s. Similar results were obtained for cooling rates as low as 10 mK/s. This grey-scale image has a full scale range of $0.25\Phi_0$ threading the sensor pickup loop (corresponding to a range in field of about 40 mG).

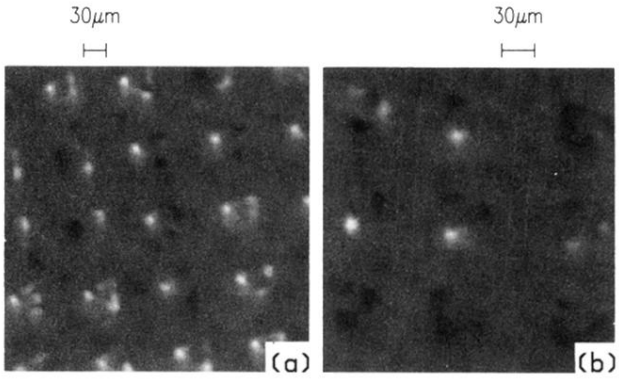

FIG. 2. Scanning SQUID micrographs of the magnetic field above the region of an array of triangular grain boundaries without (a) and with (b) superconducting material removed between the triangles [as indicated by the contrasting lines in (b)] to try to limit the effects of screening currents.

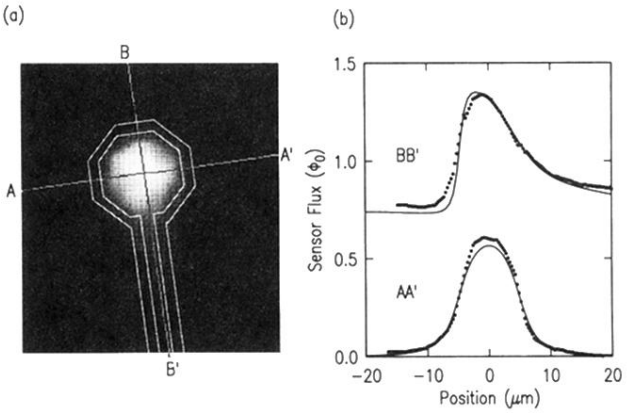

FIG. 3. (a) Abrikosov vortex trapped in the bulk of a thin film of $YBa_2Cu_3O_{7-x}$. The cross sections (dots) in (b) (the flux through the sensor loop as a function of position) are fit by assuming a total flux in the vortex of $\Phi_0 = h/2e$, with the spacing between the loop and the point of contact of the SQUID assembly as the only fitting parameter. In this geometry a bulk flux quantum (with total flux Φ_0) couples a total flux of about $0.6\Phi_0$ into the sensor loop of the SQUID.

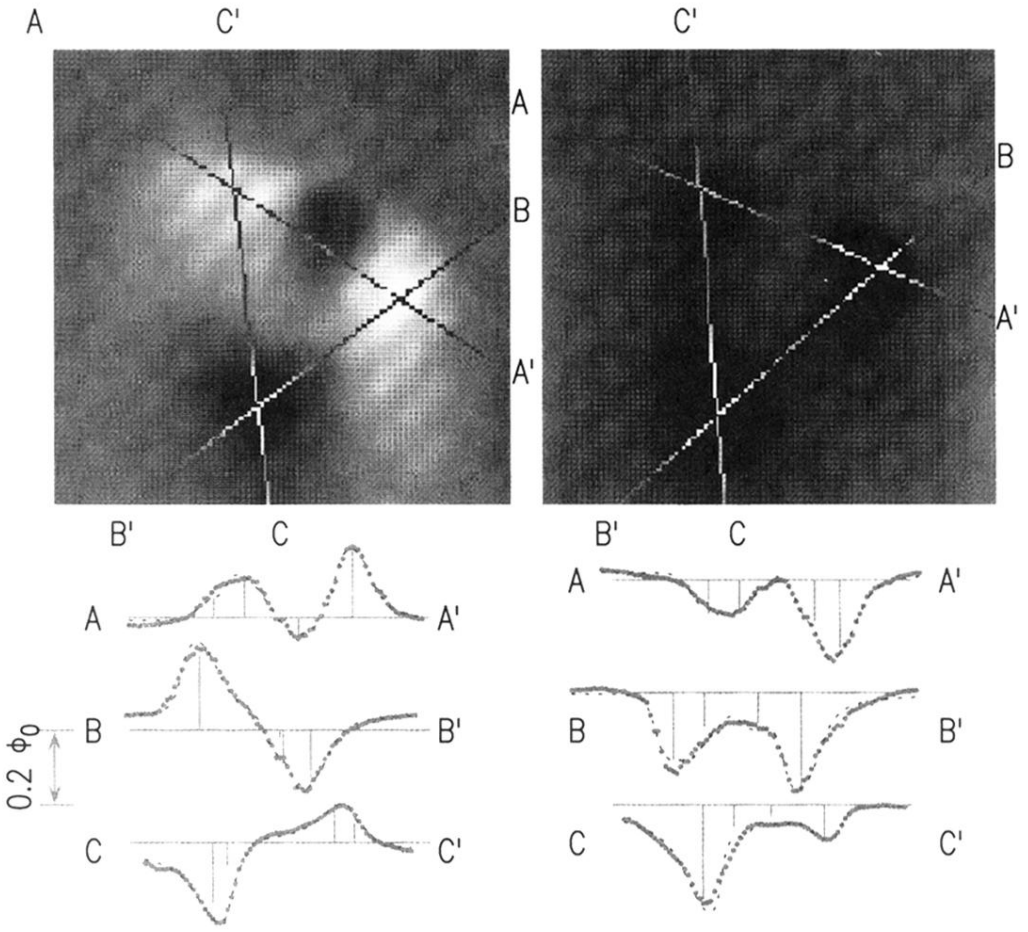

FIG. 4. The data from row 1, column 1 (left) and row 1, column 3 from Fig. 2(b) is fit using nine fractional flux vortices, each with total flux much smaller than Φ_0. The sum of the fractional charges in the left-hand fits is $0.05\Phi_0$, the sum for the right-hand fits is $-0.96\Phi_0$.